An Investigation of *in vitro* Cytotoxicity and apoptotic potential of aromatic diselenides

Masood Ahmad Rizvi, Santosh Guru, Tahira Naqvi, Manjeet Kumar, Navanath Khumbhar, Showkat Akhoon, Shazia Banday, Shashank K. Singh, Shashi Bhushan, G. Mustafa Peerzada, Bhahwal Ali Shah

PII: S0960-894X(14)00584-8
DOI: http://dx.doi.org/10.1016/j.bmcl.2014.05.075
Reference: BMCL 21689

To appear in: *Bioorganic & Medicinal Chemistry Letters*

Received Date: 19 February 2014
Revised Date: 11 May 2014
Accepted Date: 22 May 2014

Please cite this article as: Rizvi, M.A., Guru, S., Naqvi, T., Kumar, M., Khumbhar, N., Akhoon, S., Banday, S., Singh, S.K., Bhushan, S., Mustafa Peerzada, G., Shah, B.A., An Investigation of *in vitro* Cytotoxicity and apoptotic potential of aromatic diselenides, *Bioorganic & Medicinal Chemistry Letters* (2014), doi: http://dx.doi.org/10.1016/j.bmcl.2014.05.075

An Investigation of *in vitro* Cytotoxicity and apoptotic potential of aromatic diselenides

Masood Ahmad Rizvi,[a]* Santosh Guru,[b] Tahira Naqvi,[a] Manjeet Kumar,[c] Navanath Khumbhar,[d] Showkat Akhoon,[a] Shazia Banday,[a] Shashank K. Singh,[b] Shashi Bhushan,[b] G. Mustafa Peerzada[a] and Bhahwal Ali Shah[c]*

[a]*Department of Chemistry, University of Kashmir, Hazratbal, Srinagar, 190006, J&K, India.*
[b]*Division of Cancer Pharmacology, CSIR-Indian Institute of Integrative Medicine, Jammu-180001, India*
[c]*Natural Product Chemistry Division, CSIR-Indian Institute of Integrative Medicine (IIIM), Canal Road, Jammu Tawi, 180001, India.*
[d]*Institute of Bio-Informatics and Biotechnology, University of Pune, Ganeshkhind Road, Pune, 411007, India*

* Corresponding authors e-mail address: masoodku2@gmail.com (MAR); bashah@iiim.res.in (BAS)

Key words: Diselenides; anti-cancer; apoptosis; DNA-binding; *in silico*.

Introduction:

Metal complexes have been a subject of consistent investigations to develop therapeutics for treatment of human diseases particularly cancer.[1] In this regard, recent investigations ascertain the dual function of selenium compounds as chemo preventives,[2] as well as selective anti tumor therapeutics, with the induction of apoptosis and inhibition of cell proliferation as the broader mechanisms in the cancer chemoprevention.[3,4] The epidemiological studies suggest a correlation of increased risk of multi organ cancer with low levels of selenium intake or decreased plasma levels of selenium.[5] Selenium compounds in different chemical architectures target cancer in different ways and with different efficacies.[4] The toxicity concern of inorganic selenium compounds often limits their use in chemoprevention[6] even though they may be equivalent or more superior chemo preventives to organoselenium compounds.[7] In view of low toxicity, coupled with the fact that human exposure to selenium predominantly occurs through selenomethionine in food stuff, investigators are focusing on organic forms of selenium for better chemoprevention. The various pathways that have been considered in the cancer chemoprevention by organoselenium compounds include: (i) Protective role of selenoproteins (ii) induction of apoptosis (iii) immune system effects (iv) detoxification of antagonistic metals (v) inactivation of nuclear transcription factor (vi) regulation of lipoxygenases (vii) reduction of oxidative stress (viii) induction of Phase II enzymes (ix) inhibition of DNA adduct formation (x) cell cycle arrest.[8] However the significant cellular phenomenon in cancer chemoprevention by organoselenium compounds is induction of apoptosis.[3] Thus, designing organoselenium compounds can be of interest to potentiate chemotherapy by tackling problems of drug induced toxicity, drug resistance and other plethora of physiological effects in cancer chemotherapy.[9]

Therefore, in continuation of our work to develop anticancer lead molecules,[10] we report synthesis of symmetric aromatic organo diselenides (**1-13**) and their *in vitro* cytotoxicity against a panel of human cancer cell lines. The apoptotic potential of the lead compound, **8** was investigated by several end point markers of the apoptosis such as DNA damage, loss in mitochondrial membrane potential and apoptotic bodies formation using phase contrast microscopy with and without Hoechst staining. Furthermore the DNA binding ability of synthesized compounds was theoretically investigated using molecular Docking method. The present study was aimed to highlight the significance of organo diselenides in the discovery of novel anticancer agents.

Results and Discussion

Chemistry

A library of symmetric aromatic diselenides was synthesized according to Bhasin's synthetic methodology.[11] The protocol involves generating diselenide anion (Se_2^{2-}), by reducing elemental selenium with hydrazine hydrate in sodium hydroxide. The diselenide anion (Se_2^{2-}) generated in the reaction mixtures reacts *in situ* with bromo benzene derivatives to generate the corresponding diselenides. Initially elemental selenium was stirred with hydrazine and sodium hydroxide in DMF at room temperature for two hours. The bromo benzene reagents were added to the reaction mixture and further refluxed for 4 hrs in DMF around 120 ^oC, to get corresponding diselenides (scheme-1).

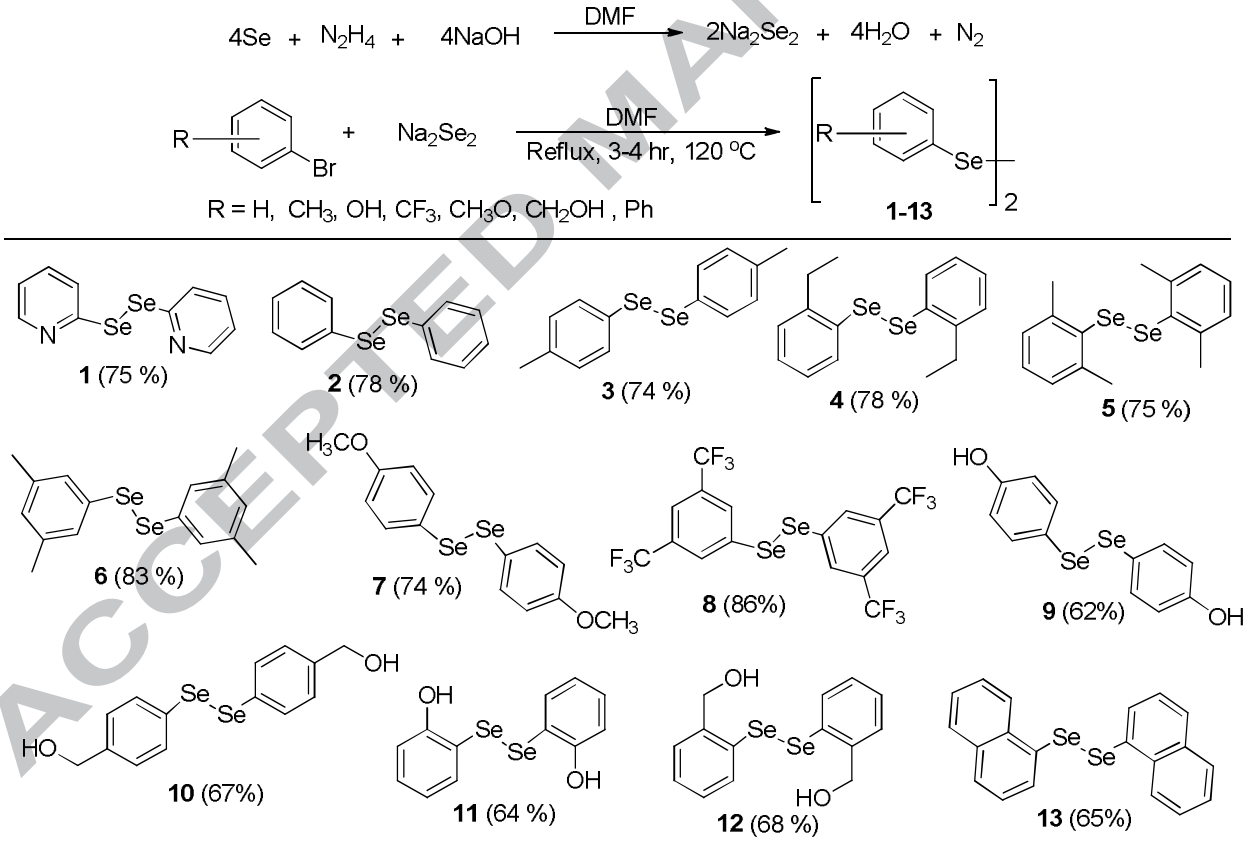

Scheme-1. Synthesis of symmetric aromatic diselenides

The reaction of un-substituted as well as methyl and ethyl substituted aryl bromides at various positions and electron rich 4-methoxy phenyl bromide gave the corresponding products in good yields (**2-7**). However, the reaction with electron withdrawing substituent like bistriflouromethyl substituted phenyl bromide give corresponding diselenide (**8**) in excellent yields (86 %). Hydroxy substitution at various positions also provides the corresponding diselenide in good yields (**9-12**). Bicyclic system like 1-napthyl bromide also (adaptable to reaction condition) gave the product in 65% yields (**13**).

Biological Activity

The synthesized diselenides (**1-13**) were screened for their ability to induce cytotoxicity against panel of human cancer cell lines viz., human promyelocytic leukemia (HL-60), human epithelial carcinoma cell line (OVCAR-5), renal cell adenocarcinoma cell line (786-O), colorectal adenocarcinoma cell line (HT-29), human prostate cancer cell line (PC-3). All the compounds displayed a range of cytotoxicity towards this cancer cell line, with the compound **8** to be the most cytotoxic (Table 1). Having an impressive cytotoxicity towards leukemia-HL-60 and prostate-PC-3 (IC_{50} value of 8 and 13 µM) we further explored **8** for its cytotoxicity potential against breast cancer-MCF-7, pancreatic cancer-MIA-PA-Ca-2 and colon cancer- HCT-116, cell lines. The IC_{50} values of **8** in MCF-7, MIA-Pa-Ca-2 & HCT-116 cells were 18, 25 and 27 µM respectively. Furthermore, the time dependent (6, 12, 24 and 48 h) cytotoxic studies of **8** on HL-60 cell line indicate the progressive decrease in IC_{50} values with increasing time (Figure 2).

Table 1. Inhibition of cell proliferation by compounds **1-13** against a panel of human cancer cell lines

Compound	IC 50 (µM) in different Human Cancer cell lines				
	Leukemia	**Epithelial**	**Renal**	**Colorectal**	**Prostate**
	HL-60	**OVCAR-5**	**786-O**	**HT-29**	**PC-3**
1	28	27	29	30	26
2	32	38	38	31	42
3	33	31	29	37	29
4	28	38	42	56	43
5	27	39	40	35	33

6	23	34	33	36	30
7	12	26	28	24	27
8	**8**	**20**	**24**	**21**	**13**
9	13	27	33	37	29
10	11	24	30	27	26
11	14	21	27	23	25
12	14	16	27	25	28
13	16	25	32	34	40

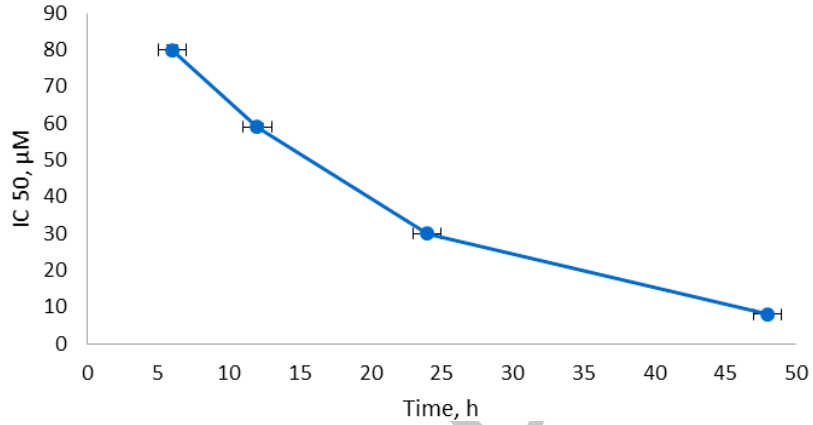

Figure 2. Time dependent cytotoxic profile of **8** on HL-60 cell line. Data is Mean ± SD (n= 8 wells), and representative of one of three concordant experiments. Initially, cells were incubated with MTT solution for 4 hr and optical density of formazon crystals was measured as described in experimental procedures.

DNA Cell Cycle Analysis

The good cytotoxic behavior of **8** towards HL-60 cells (IC_{50} value of 8µM), encouraged us to choose this cell line for DNA cell cycle analysis. The cell cycle is a fundamental and ordered event in which DNA replicates, and homologous chromosomes segregate and get equally distributed among the daughter cells. Deregulated cell cycle is one of the major hallmarks of cancer cells. These cells may lose the ability to regulate the cell cycle and control their rate of proliferation. A rate-limiting step in the cell cycle that is often disturbed in cancer is the progression of cells through the first gap (G1) phase. Many anticancer drugs act by blocking one or more stages of the cell cycle and eventually trigger apoptosis. The effect of antiproliferative

agent on cell cycle progression and DNA damage appears to depend on concentration of the compound and duration of the treatment. Increased resistance to apoptosis is a characteristic of many tumor cells. Therefore, apoptosis deficiency is considered to be a major cause of the therapeutic resistance of tumors in the clinic, since many chemo-and radio therapeutic agents' act through the induction of apoptosis. HL-60 cells when exposed to **8** at concentration of 10, 20 and 30 µM for 24 h exhibited an increase in apoptosis percentage in dose dependent manner i.e., 2, 5 and 24% sequentially (Figure 3). Interestingly, compound delay the s-phase of cell cycle with concurrent induction of apoptosis in HL-60 cells.

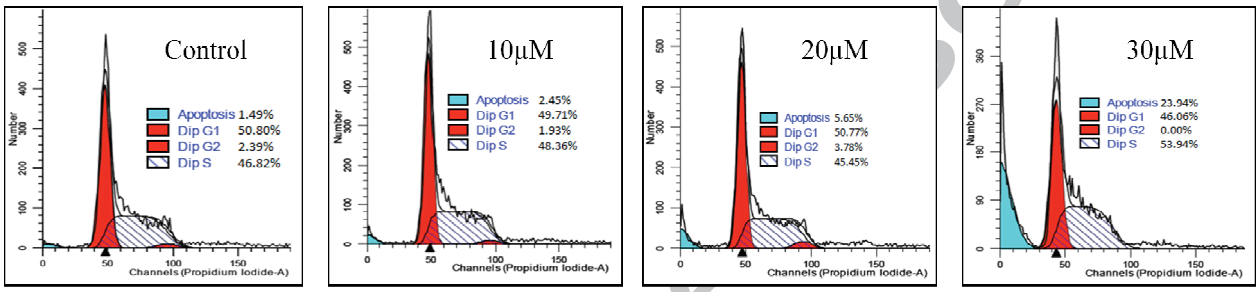

Figure 3. DNA cell cycle analyses of HL-60 cells exposed to specified concentration of **8** for 24 hr. After treatment cells were stained with Propidium iodide, PI (10µg/mL) to determine DNA fluorescence and cell cycle phase distribution as described in experimental procedures. Data was analyzed by Modfit software (Verity Software House Inc., Topsham, ME) for the proportions of different cell cycle phases. The fraction of cells from apoptosis, G1, S and G2 phases analyzed from FL2- A vs. cell counts are shown in %.

Measurement of Mitochondrial Membrane Potential

The alteration of the mitochondrial function plays a major role in the apoptotic process. The loss of mitochondrial membrane potential (Ψ_{mt}) leads to depolarization of mitochondrial membranes and mitochondrial dysfunction leading to cell death. We investigated the effects of **8** on the mitochondrial potential of HL-60 treated cells. This was examined by measuring their ability to retain Rhodamine 123, a fluorescent dye used to indicate the loss of mitochondrial transmembrane potential. Under this condition, the control HL-60 cells showed 6% loss of Ψ_{mt}, which increase to 58% after the treatment of **8**. It induced the loss of mitochondrial membrane potential (MMP) in HL-60 cells in a dose dependant manner (Figure 4). The loss of

mitochondrial membrane potential also releases several pro-apoptotic factors that activate caspases and finally induces apoptosis.

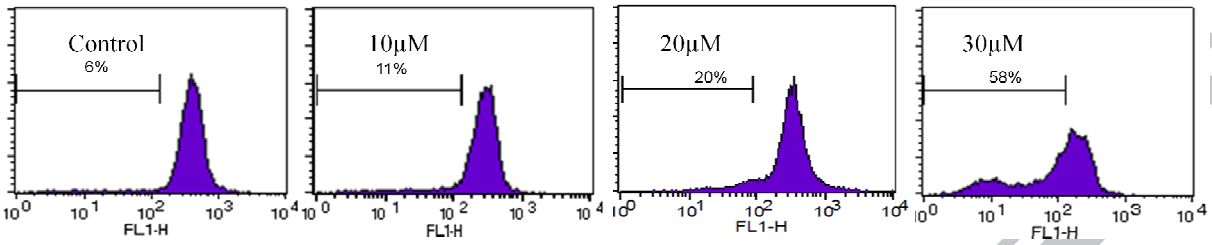

Figure 4. Mitochondrial membrane potential analyses was performed on HL-60 cells exposed to specified concentration of **8** for 24 h. After treatment cells were stained with Rhodamine 123 dye (200 nm) for 40 min to determine membrane potential as described in experimental procedures. Data was analyzed by Cell Quest Pro software from BD Biosciences. Data were representative of one of three similar experiments.

Apoptotic morphological alteration induce by 8

The characteristic apoptotic morphological changes of HL-60 treated cells were assessed by the fluorescent microcopy after staining with Hoechst dye. Because of the integrity of the cell plasma membrane, Hoechst dye was unable to infiltrate into the HL-60 cells when the cells were alive or still in the early process of apoptosis, while the dead cells had Hoechst inside and the nuclei were stained a bright blue color. The results revealed nuclear condensation, membrane blebbing, nuclear fragmentation and apoptotic bodies (the characteristic of apoptosis) in cells that had been incubated with **8** (Figure 5). The control cells did not exhibit any of the above morphological changes, the nuclei were stained a less bright blue and the color was homogeneous. Chromatin condensation and other apoptotic characters were observed only in the treated cells. Compound **8** at 20 and 30 μM concentrations significantly induced morphological characteristics similar to those of apoptotic cells when observed under phase contrast inverted microscopy as well as nuclear staining through the Hoechst fluorescent dye (Figure 5).

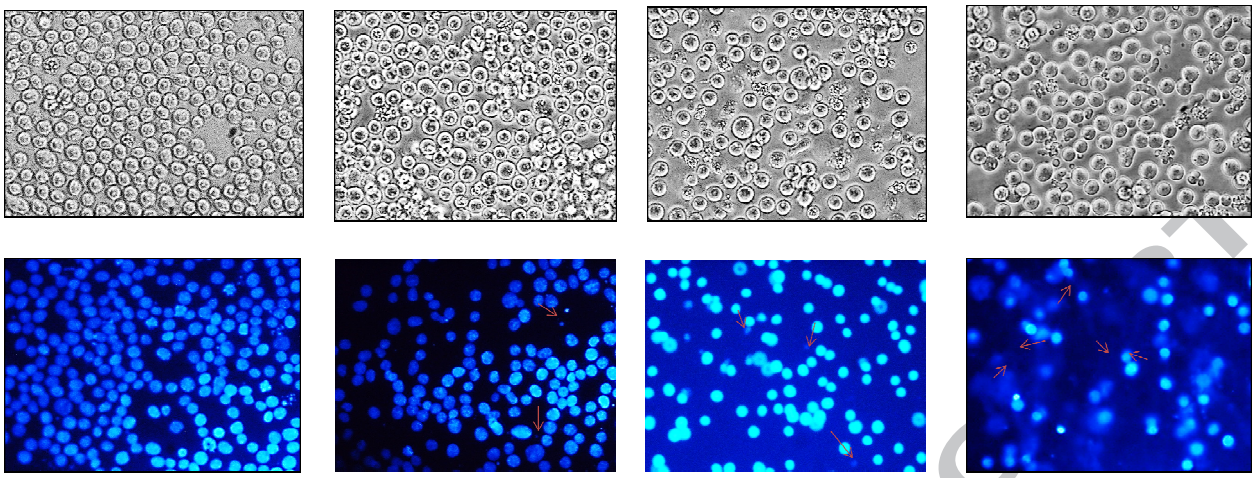

Figure 5. Effect of **8** on the cellular and nuclear morphology of HL-60 cells. Cells were treated with 10, 20 & 30μM concentrations of **8** for 24 h, visualized for cellular morphology and simultaneously stained with DNA binding Hoechst 33258 dye as described in experimental procedures. Nuclear morphology and apoptotic bodies' formation were visualized on fluorescent microscope. Condensed nuclei and the apoptotic bodies are indicated by red arrows. Data are representative of one of three similar experiments and magnification of the pictures was 30X on Olympus 1X 70 inverted microscope.

In Silico DNA Binding study of 8

Molecular docking and other molecular dynamics simulation algorithms are attractive tools to theoretically understand the magnitude of binding and mode of interaction in the ligand–receptor complexes.[12] Corroborating experimental results which are a net outcome of all the parameters in a blend with theoretical calculations can be impressive for the step to step analysis and prediction of lead compounds in a time and cost effective manner.[13] Prompted by a good apoptotic behavior of **8**, we attempted to explore its DNA binding ability through molecular docking studies. In order to locate the binding site of **8** on DNA molecule, we did initial surface docking. After optimizing for the grid size of **8** binding site on DNA, re-docking was done using the discussed procedure (please see experimental procedures). The lowest energy docked complex of DNA-compound **8** is depicted in Figure 6. The **8** selectively binds to minor groove of DNA, where it is stabilized by various Vander Waal type and hydrophobic interactions with DNA. One benzene ring of **8** is interacting with G-C rich region including $G22_B$, $G4_A$ and $C21_B$ bases whereas other

benzene ring is stacked with A-T rich region containing nucleotide bases such as $A6_A$, $T7_A$ and $T20_B$ (Figure 7). The fluorine atoms of **8** are involved in intermolecular hydrogen bonding interactions with $G22_B$ and $G4_A$ of opposite chain bases. Hydrogen bonding interactions such as F1….HN(2)$G22_B$, F1….HN(2)$G4_A$, F2….HC1'$G22_B$, F5….HC5'$G22_B$, F10….HC(2)$A6_A$, F11…HC4'$T7_A$, F12….HC1'$T20_B$ and F12…HC5'$C21_B$ are providing stability to compound **8**-DNA complex. The lowest binding energy of -6.62 Kcal mol^{-1} and above mentioned hydrogen bonding interactions are indicative that **8** efficiently binds to the DNA molecule by positioning in stacked orientation within DNA molecule. The molecular docking results are predictive of the DNA binding potential of the **8**.

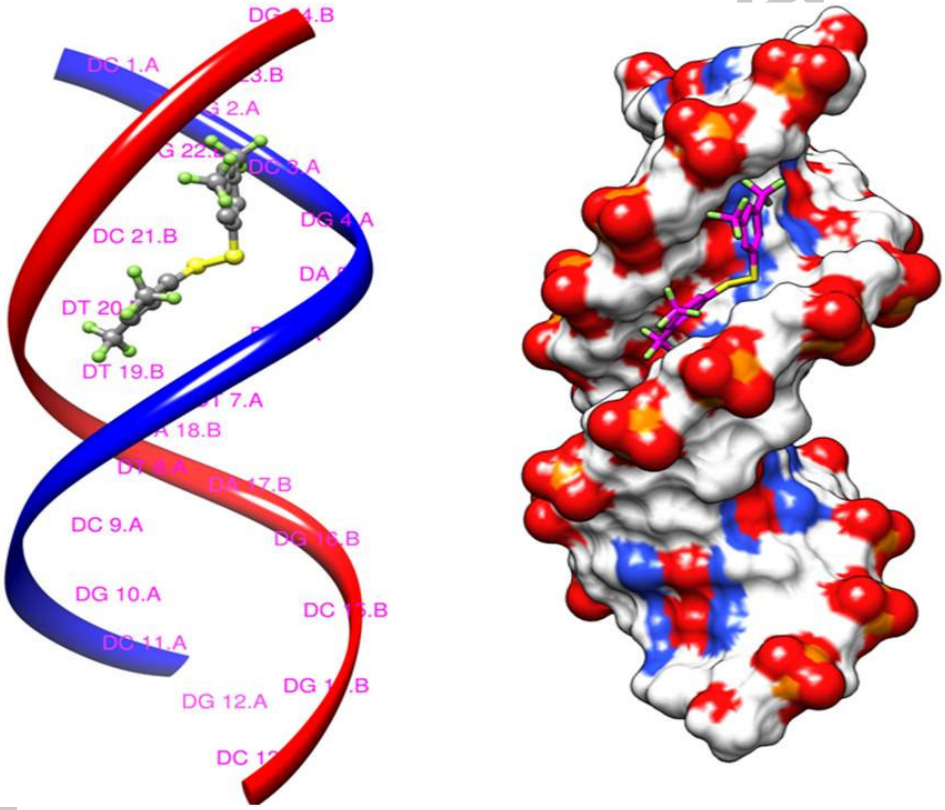

Figure 6: Docked view of compound **8** with DNA dodecamer (1BNA.pdb): a) Ribbon model of compound **8** in minor groove of DNA. b) Surface area of compound **8** with DNA dodecamer.

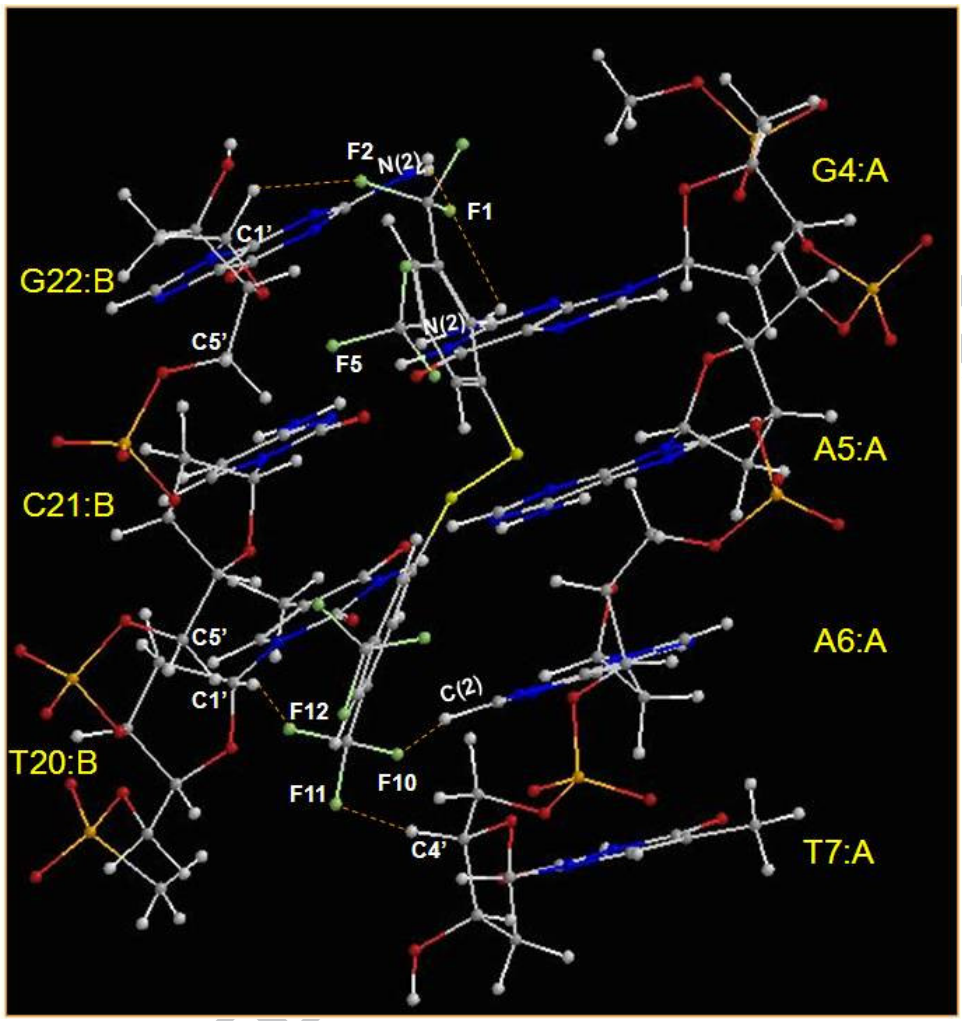

Figure 7: Intermolecular hydrogen bonding interactions between compound **8** and DNA dodecamer.

Conclusion

Our findings showed that all the synthesized diselelenides (**1-13**) showed promising cytotoxicity against human cancer cells lines. Compound **8** was found to be the most active and showed pro-apoptotic effects evidenced by various biological end points like DNA damage with s-phase delay, loss in mitochondrial membrane potential and apoptotic bodies formation. *In silico* DNA binding studies suggested that **8** selectively binds to minor groove of DNA, where it is stabilized by hydrogen bonding and hydrophobic interactions with DNA. Further studies aimed at the detailed molecular mode of action of compound **8** are underway. Moreover, efforts are continued

towards synthesizing library of selenides to develop anticancer leads and thereby a moiety of therapeutic significance.

General Experimental Procedures

^{1}H and ^{13}C NMR spectra in $CDCl_3$ were recorded on 400 MHz spectrometers with TMS as an internal standard. Chemical shifts are expressed in parts per million (δ ppm); J values are given in Hertz. Reagents and solvents used were mostly AR grade. Silica gel aluminum plates were used for TLC. HRMS were recorded on UHD LC/MS Q-TOF. The RPMI-1640 medium, Minimum essential medium (MEM), Dulbecco's Modified Eagles Medium (DMEM), fetal Calf Serum (FCS), penicillin, streptomycin, L-Glutamine, pyruvic acid, trypsin, gentamycin, penicillin, sulforhodamine blue (SRB), 3-[4,5-dimethylthiazol-2-yl]-2,5-diphenyl]-tetrazolium bromide (MTT), $NaHCO_3$, propidium iodide (PI), DNase-free RNase and dimethyl sulphoxide (DMSO) were purchased from Sigma Aldrich, USA. All other reagents were AR graded and available locally.

General procedure for Synthesis of Diselenides: To a rapidly stirred solution of sodium hydroxide (1.52 g, 38 mmol) and selenium powder (1.98 g, 25 mmol) in dimethylformamide (100 mL) was added 100% hydrazine hydrate (1 mL, 25 mmol) dropwise at room temperature (r.t.). The mixture was stirred for two hours. 2-bromo pyridine (3.92 g, 25 mmol) was added drop-wise to the reaction mixture and refluxed for four hours. After the consumption of whole reactant as evidenced by TLC, the reaction was stopped and diluted with water. The extraction was done with ethyl acetate and the organic layer was dried with Na_2SO_4. The solvent was removed on a rota-evaporator and the residue was purified by column chromatography to give to give 1,2-di(pyridine-2-yl)diselane (**1**) in 75% yields. In a similar manner the other diselenides were prepared using appropriate amounts of bromo benzene reactants under same procedure.

1,2-di(pyridine-2-yl)diselane (1): Yield 75 %; Spectroscopic data was in good agreement with literature data reported earlier.[14] ^{1}H NMR (500 MHz, $CDCl_3$): 6.98 (d, 2H, J = 4.7), 7.51 (m, 2H), 7.75 (d, 2H, J = 7.4), 8.40 (s, 2H); ^{13}C NMR (100 MHz, $CDCl_3$): 154.8, 149.5, 137.1, 123.5, 120.2; HRMS calcd. for $C_{10}H_9N_2Se_2$ $[M+H]^+$ 316.9091, found 316.90004.

1,2-diphenylselane (2): Yield 78 %; Spectroscopic data was in good agreement with literature data reported earlier.[15] ^{1}H NMR (500 MHz, $CDCl_3$) δ 7.62 – 7.34 (m, 4H), 7.32 – 6.99 (m, 6H); ^{13}C NMR (100 MHz, $CDCl_3$) δ 132.7, 131.9, 130.8, 127.6; HRMS calcd. for $C_{12}H_{11}Se_2$ $[M+H]^+$ 314.9186, found 314.9210.

1,2-bis(4-methylphenyl)diselane (3): Yield 74 %; Spectroscopic data was in good agreement with literature data reported earlier.[15] ^{1}H NMR (500 MHz, $CDCl_3$) δ 7.45 (d, 4H, J = 8.4 Hz), 7.10 (d, 4H, J = 8.4 Hz), 2.32 (s, 6H); ^{13}C NMR (100 MHz, $CDCl_3$) δ 139.9, 133.7, 130.9, 127.9, 23.1; HRMS calcd. for $C_{14}H_{15}Se_2$ $[M+H]^+$ 342.9499, found 342.9486.

1,2-bis(2-ethylphenyl)diselane (4): Yield 78 %; Spectroscopic data was in good agreement with literature data reported earlier.[16] ^{1}H NMR (500 MHz, $CDCl_3$) δ 7. 87 – 7.62 (m, 2H), 7.35 – 7.29 (m, 2H), 7.28 – 7.20 (m, 2H), 7.19 – 7.05 (m, 2H), 2.51 – 2.22 (m, 4H), 1.40 – 1.17 (m, 6H); ^{13}C NMR (100 MHz, $CDCl_3$) δ 148.2, 134.4, 130.8, 127.1, 126.6, 125.6, 27.7, 13.5; HRMS calcd. for $C_{16}H_{19}Se_2$ $[M+H]^+$ 370.9812, found 370.9870.

1,2-bis(2,6-dimethylphenyl)diselane (5): Yield 75 %; ^{1}H NMR (500 MHz, $CDCl_3$) δ 7.51 – 7.19 (m, 2H), 7.19 – 6.89 (m, 4H), 2.53 – 2.10 (m, 12H); ^{13}C NMR (100 MHz, $CDCl_3$) δ 142.8, 127.3, 126.4, 23.1; HRMS calcd. for $C_{16}H_{19}Se_2$ $[M+H]^+$ 370.9812, found 370.9862.

1,2-bis(3,5-dimethylphenyl)diselane (6): Yield 83 %; Spectroscopic data was in good agreement with literature data reported earlier.[17] ^{1}H NMR (500 MHz, $CDCl_3$) δ 7.34 – 7.29 (m, 2H), 7.42 – 7.24 (m, 2H), 7.01 – 6.97 (m, 1H), 7.07 – 6.87 (m, 1H), 2.35 – 2.31 (m, 12H); ^{13}C NMR (100 MHz, $CDCl_3$) δ 144.8, 138.5, 130.1, 128.5, 21.9; HRMS calcd. for $C_{16}H_{19}Se_2$ $[M+H]^+$ 370.9812, found 370.9810.

1,2-bis(4-methoxyphenyl)diselane (7): Yield 74 %; Spectroscopic data was in good agreement with literature data reported earlier.[15] ^{1}H NMR (500 MHz, $CDCl_3$): 7.52 (d, 4H, *J* = 8.5), 6.81 (d, 4H, *J* = 8.5), 3.79 (s, 6H); ^{13}C NMR (100 MHz, $CDCl_3$): 160.1, 138.5, 134.7, 114.5, 55.3; HRMS calcd. for $C_{16}H_{15}Se_2$ $[M+H]^+$ 374.9397, found 374.9405.

1,2-bis(3,5-bis(trifluoromethyl)phenyl)diselane (8): Yield 86 %; ^{1}H NMR (500 MHz, $CDCl_3$): 7.73-7.91 (m, 4H), 7.99-8.03 (d, 2H, *J* = 6.9); ^{13}C NMR (100 MHz, $CDCl_3$): 121.4, 122.4, 131.6, 131.7, 132.9; HRMS calcd. for $C_{16}H_7F_{12}Se_2$ $[M+H]^+$ 586.8681, found 586.8620.

1,2-bis(4-hydxoxyphenyl)diselane (9): Yield 62 %; Spectroscopic data was in good agreement with literature data reported earlier.[18] ^{1}H NMR (500 MHz, $CDCl_3$): 7.36 (m, 4H). 6.69 (m, 4H); ^{13}C NMR (100 MHz, $CDCl_3$): 155.3, 134.8, 122.1, 116.3; HRMS calcd. for $C_{12}H_{11}O_2Se_2$ $[M+H]^+$ 346.9084, found 346.9101.

(Diselanediylbis(1,4-phenylene))dimethanol (10): Yield 67 %; Spectroscopic data was in good agreement with literature data reported earlier.[19] ^{1}H NMR (500 MHz, $CDCl_3$): 7.50 (d, 4H, J = 7.3), 7.25(d, 4H, J = 7.7), 4.64 (s, 4H); ^{13}C NMR (100 MHz, $CDCl_3$): 139.8, 133.1, 128.5, 127.4, 64.5; HRMS calcd. for $C_{14}H_{15}O_2Se_2$ $[M+H]^+$ 374.9397, found 374.9362.

1,2-bis(2-hydroxyphenyl)diselane (11): Yield 64 %; Spectroscopic data was in good agreement with literature data reported earlier.[15] ^{1}H NMR (500 MHz, $CDCl_3$) δ 7.63 – 7.49 (m, 2H), 7.45 – 7.40 (m, 1H), 7.39 – 7.35 (m, 1H), 7.01 – 6.80 (m, 2H), 6.78 – 6.74 (m, 2H); ^{13}C NMR (100 MHz, $CDCl_3$) δ 157.3, 135.1, 127.9, 120.8, 115.7, 108.6; HRMS calcd. for $C_{12}H_{11}O_2Se_2$ $[M+H]^+$ 346.9084, found 346.9110.

(Diselanediylbis(1,2-phenylene))dimethanol (12): Yield 68 %; ^{1}H NMR (500 MHz, $CDCl_3$) δ 7.77 – 7.64 (m, 2H), 7.51 – 7.34 (m, 2H), 7.34 – 7.12 (m, 4H), 4.91 – 4.62 (m, 4H); ^{13}C NMR (100 MHz, $CDCl_3$) δ 141.5, 134.8, 134.2, 127.5, 126.6, 125.9, 63.8; HRMS calcd. for $C_{14}H_{15}O_2Se_2$ $[M+H]^+$ 374.9397, found 374.9428.

1,2-bis(naphthalen-1-yl)diselane (13): Yield 65 %; Spectroscopic data was in good agreement with literature data reported earlier.[20] ^{1}H NMR (400 MHz, $CDCl_3$): 7.83-7.76 (m, 2H) 7.55-7.48 (m, 4H) 7.37-7.31 (m, 4H) 7.29-7.25 (m, 2H), 7.21-7.15 (m, 2H); ^{13}C NMR (100 MHz,$CDCl_3$): 134.2, 131.8, 128.8, 128.3, 126.6, 126.4, 125.6; HRMS calcd. for $C_{20}H_{15}Se_2$ $[M+H]^+$ 414.9499, found 414.9524.

Cell culture, growth conditions and treatments: Human Prostate Cancer cells PC-3, Breast Cancer cell MCF-7, Leukemia Cells HL-60, pancreatic cancer cell MIA-Pa-Ca-2 and colon cancer cells HCT-116 were obtained from European Collection of Cell Cultures (ECACC). The PC-3, MCF-7 and HCT-116 cells were grown in Minimum essential medium (MEM), MIA-Pa-Ca-2 cells were grown in Dulbecco's Modified Eagle's Medium (DMEM) and HL-60 Cells were grown in RPMI-1640 medium supplemented with 10% heat inactivated fetal bovine serum (FBS), penicillin (100 units/ml), streptomycin (100 µg/ml), L-glutamine (0.3 mg/mL) and

$NaHCO_3$(8mg/mL). Cells were grown in an atmosphere of 5% CO_2 and 95% relative humidity in a CO_2 incubator (Thermocon Electron Corporation, USA) at 37°C. Adherent cultures were harvested by trypsinaization (0.05% trypsin , 0.02% EDTA in PBS). Soon after cells were ready to detach, 5ml of medium were added to stop trypsinization. Cells were dispersed gently by pipetting incomplete growth medium, centrifuged at 1000 rpm, for 5 min. On the other hand, suspension cultures (HL-60) were harvested by centrifugation for 5 min at 1000 rpm. Different molecules used in this study were dissolved in DMSO and were delivered to cell cultures in complete medium. Since DMSO is cytotoxic at high concentrations therefore its final concentration in the cells was below 1% w/v.

Cell Proliferation Assay Using MTT: This assay is a quantitative colorimetric method for the determination of cell survival and proliferation. The assessed parameter is the metabolic activity of viable cells. Metabolically active cells reduce pale yellow tetrazolium salt (MTT) to a dark blue water-insoluble formazan, which can be, after solubilization with DMSO, directly quantified. The absorbance of the formazan directly correlates to the number of viable cells. The different human cancer cell lines HL-60, PC-3, MIA-Pa-Ca-2, MCF-7 and HCT-116 cells were plated in 96-well plates at a density of 6000 cell/well in 100µL of medium. The cell cultures were incubated with different concentrations of test material and incubated for 48 hr. The MTT dye at a concentration of 2.5mg/mL [3-(4, 5-dimethylthiazol-2-yl)-2, 5-diphenyltetrazolium bromide] was added for 4 hr. The supernatant was aspirated and MTT-formazon crystals dissolved in 150µL of DMSO; OD was measured at λ540 (reference wavelength, λ620) on an ELISA reader (BioTek.). Cell growth was calculated by comparing the absorbance of treated versus untreated cells.[21]

Cell cycle analysis: DNA fragmentation constitutes one biochemical hallmark of apoptosis. Thus, measurement of DNA content makes it possible to identify apoptotic cells, to recognize the cell cycle Phase specificity, and to quantify apoptosis. For flow cytometry analysis of the relative nuclear DNA content, the fluorescent dye propidium iodide (PI), which becomes highly fluorescent after binding to DNA, is most commonly used. After permeabilization, PI binds to DNA in cells at all stages of the cell cycle, and the intensity with which a cell nucleus emits fluorescent light is directly proportional to its DNA content. HL-60 cells (2×10^6 /3ml/well) in 6-well plate were treated with different concentrations of test material for 24 hr. The cells were

harvested and centrifuged at 400 g for 5 min. The supernatant discarded and the pellet washed twice with 2 ml PBS. The cells were fixed overnight in 1 ml chilled 70% ethanol in PBS at 4ºC. Cell washed twice with 2 ml PBS, cell suspension was incubated with RNase digestion (400µg/ml) at 37ºC for 1 hr. Finally, cells were stained with PI (10 µg/ml) for 30 min in dark and analyzed immediately for DNA content on Flow Cytometer. Cell cycle histograms were analysed using the ModFit LT™ 3.2.1 software packages. In this program, debris and single cell populations are gated out using two parameter histogram of FL2-A versus FL2-W. The fluorescence intensity of sub-G0 cell fraction represents the apoptotic cell population.[22]

Mitochondrial membrane potential (MMP) assay: HL-60 cells ($1x10^6$ cells/2mL/well) were treated with compound **8** at different concentrations for 24h. Thirty minutes before the end of the experiment, the cell culture was treated with Rhodamine-123 (200nM) and keep in the dark for 30 mn. Cells were then collected, centrifuged (400g; 4^oC; 5min), the pellet was washed with 1 ml of PBS and centrifuge as mentioned earlier. The fluorescence intensity of 10,000 events was analyzed in FL-1 channel on BD FACSCalibur (Becton Dickinson, USA) flow cytometer. The decrease in fluorescence intensity because of mitochondrial membrane potential loss was analyzed in FL-1 channel and the change of in potential membrane ($\Delta\psi m$) was assessed by comparing fluorescence.[22]

Hoechst 33258 staining of cells for nuclear morphology: HL-60 cells were treated with indicated concentrations of compound **8** (10, 20 & 30µM) for 24 hr. Cells were centrifuged at 400 g for 5min and washed twice with PBS. Cells were then stained with one milliliter of staining solution (Hoechst 33258, 10 µg/mL of 0.01M citric acid and 0.45 M disodium phosphate containing 0.05% Tween 20) under subdued light at room temperature. After staining, the cells were resuspended in 50µL of mounting fluid (PBS: glycerol, 1/1), 10 µL mounting solution, containing cells was spread on clean glass slides and covered with the cover slips. The slides were then observed for any nuclear morphological alterations and apoptotic bodies under inverted fluorescence microscope (Olympus 1X70, magnification 30X) using UV excitation.[23]

***In silico* study of 8:** The crystal structure of DNA dodecamer (1BNA.pdb) having sequence d(CpGpCpGpApApTpTpCpGpCpG)[24] was downloaded from protein data bank (www.rcsb.org) for molecular docking studies with **8**. The geometry optimization of **8** was done by semi-

empirical PM3 method[25] using *Spartan Pro 6.1.0* software.[26] While as Autodock 4.2 software was used for Molecular docking studies.[27] Prior to docking studies, DNA structure was refined by removing non-polar hydrogen atoms and adding Kollman united atom charges and polar hydrogen atoms. Gasteiger charges and hydrogen atoms were added to the **8** using Autodock wizard.[27] AutoGrid module was used for calculating the grid maps centered on the ligand (**8**) binding site of DNA. The grid size was set to 50 A° × 50 A° × 62 A° with a grid spacing 0.375 A°. The step size of 1Å for translation and the maximum number of energy evaluation was set to 2,500,000. The 50 runs were performed. For each of the 50 independent runs, a maximum number of 2,70,000 LGA operations were generated on a single population of 150 individuals. The operator weights for crossover, mutation and elitism were maintained as default parameters (0.80, 0.02, and 1, respectively). The resulting 50 docked conformations were analyzed for binding energy, intermolecular energy and internal energy using Autodock wizard.[27] The DNA-compound **8** complex with lowest binding energy was used for analysis of hydrogen bonding, hydrophobic and hydrophilic interactions. Chimera software was used to generate pictorial presentation of selected docked conformation.[28]

Acknowledgments

SG and MK thank CSIR for the award of Senior Research Fellowship.

References:

1 (a) Chan, D.-H.; Lee, H.-M.; Yang, F.; Che, C.-M.; Wong, C. L.; Abagyan, R.; Leung, C.-H.; Ma, D.-L. Angew. Chem. Int. Ed. 2010, 49, 2860–2864. (b) Leung, C. H..; Zhong, H. J.; Yang, H.; Cheng, Z.; Chan, D. S.-H.; Ma, V. P. Y.; Abagyan, R.; Wong, C. Y.; Ma, D.-L. Angew. Chem. Int. Ed. 2012, 51, 9010–9014. (c) Ma, D.-L., He, H.-Z., Leung, K.-H., Chan, D. S.-H.; Leung, C.-H. Angew. Chem. Int. Ed. 2013, 52, 7666–7682

2 (a) Zeng, H.; Combs, G. F. J. Nutr. Biochem. 2008, 19, 1-7; (b) Tsavachidou, D.; McDonnell, T. J. J. Natl. Cancer Inst. 2009, 101, 306-320; (c) Jung, H. J. Seo, Y. R. Biofactors 2010, 36, 153–158; (d) Schrauzer, G. N. Crit. Rev. Biotechnol. 2009, 29, 10-17.

3 (a) Soriano-Garcia, M. Curr. Med. Chem. 2004, 11, 1657-1669; (b) Brozmanova, J.; Manikova, D.; Vlckova, V.; Chovanec, M. Arch. Toxicol. 2010, 84, 919-938.

4 Sinha, R.; El-Bayoumy, K. Curr. Cancer Drug Targets 2004, 4, 13-28.

5 Brooks, J. D.; Metter, E. J. J. Urology 2001, 166, 2034-2038.

6 Buell, D. N. Semin.Oncol. 1983, 10, 311-321.

7 (a) Ronai, Z. E.; Tillotson, J. K. Int. J. Cancer 1995, 63, 428-434; (b) Thompson, H. J.; Meeker, L. D. Cancer Res. 1984, 44, 2803-2806.

8 Naithani, R. Mini-Rev. Med. Chem. 2008, 8, 657-668.

9 Cheung-Ong, K.; Giaever, G.; Nislow, C. Chem. Biol. 2013, 20, 648-659.

10 (a) Shah, B. A.; Kaur, R.; Gupta, P.; Kumar, A.; Sethi, V. K.; Andotra, S. S.; Singh, J.; Saxena, A. K.; Taneja, S. C. Bioorg. Med. Chem. Lett. 2009, 19, 4394-4398; (b) Chashoo, G.; Singh, S.; K.; Sharma, P. R.; Mondhe, D. M.; Hamid, A.; Saxena, A.; Andotra, S. S.; Shah, B. A.; Qazi, N. A.; Taneja, S. C.; Saxena, A. K. Chem. Biol. Interact. 2011, 15, 60-71; (c) Qurishi, Y.; Hamid, A.; Sharma, P. R.; Wani, Z. A.; Mondhe, D. M.; Singh, S. K.; Zargar, M. A.; Andotra, S. S.; Shah, B. A.; Taneja, S. C.; Saxena, A. K. Future Oncol. 2012, 8, 867-81; (d) Kumar, M.; Qadri, M.; Sharma, P. R.; Kumar, A.; Andotra, S. S.; Kaur, T.; Kapoor, K.; Gupta, V. K.; Kant, R.; Hamid, A.; Johri, S.; Taneja, S. C.; Vishwakarma, R. A.; Hassan, S. R.; Shah, B. A. J. Nat. Prod. 2013, 76, 194-199; (e) Devari, S.; Jaglan, S.; Kumar, M.; Deshidi, R.; Guru, S.; Bhushan, S.; Kushwaha, M.; Gupta, A. P.; Gandhi, S. G.; Sharma, J. P.; Taneja, S. C.; Vishwakarma, R. A.; Shah, B. A. Phytochemistry 2014, 98, 183–189.

11 Bhasin, K. K.; Singh, J. J. Organomet. Chem. 2002, 658, 71-80.

12 (a) Ma, D.-L.; Chan, D. S.-H.; Leung, C.-H. Chem. Soc. Rev. 2013, 42, 2130-2141; (b) Ma, D.-L.; Chan, D. S.-H.; Leung, C.-H. Chem. Sci., 2011,2, 1656-1665.

13 Smith, J. R.; Evans, K. J.; Wright, A.; Willows, R. D.; Jamie, J. F.; Griffith, R. Bioorg. Med. Chem. 2012, 20, 1354-1363.

14 Bhasin, K. K.; Singh, J. J. Organomet. Chem. 2002, 658, 71-76.

15 Singh, D.; Deobald, A. M.; Camargo, L. R. S.; Tabarelli, G.; Rodrigues, O. E. D.; Braga, A. L. Org. Lett. 2010, 12, 3288-3291.

16 Maxwell, W. M.; Wynne, K. J. Inorganic Chemistry, 1981, 20, 1707-1712.

17 Wang, J-X.; Xi, Y.; Wu, X.; Hu, Y.; Du, Z. Synth. Commun. 1998, 28, 4619-4627.

18 Shen, L.; Shin, K-M.; Lee, K-T.; Jeong, J-H. Arch. Pharmcal Res. 2004, 27, 816-819.

19 Tripathi, S. K.; Patel, U.; Roy, D.; Sunoj, R. B.; Singh, H. B.; Wolmershaeuser, G.; Butcher, R. J. J. Org. Chem. 2005, 70, 9237-9247.

20 Li, Z.; Ke, F.; Deng, H.; Xu, H.; Xianga, H.; Zhou, X. Org. Biomol. Chem. 2013, 11, 2943-2946.

21 Kumar, A.; Malik, F.; Bhushan, S.; Sethi, V. K.; Shahi, A. K.; Kaur, J.; Taneja, S. C.; Qazi, G. N.; Singh, J. Chem. Biol. Interact. 2008, 171, 332-347.

22 Bhushan, S.; Singh, J.; Rao, M. J.; Saxena, A. K.; Qazi, G. N. Nitric Oxide 2006, 14, 7288-7293.

23 Bhushan, S.; Kumar, A.; Malik, F.; Andotra, S. S.; Sethi, V. K.; Kaur, I. P.; Taneja, S. C.; Qazi, G. N.; Singh, J. Apoptosis 2007, 12, 1911-1926.

24 Drew, H. R.; Wing, R. M.; Takano, T.; Broka, C.; Tanaka, S.; Itakura, K.; Dickerson, R. E. Proc. Natl. Acad. Sci. USA. 1981, 78, 2179-2183.

25 (a) Stewart, J. J. P. J. Comput. Chem. 1991, 12, 320-341; (b) Kumbhar, N. M.; Sonawane, K. D. J. Mol. Graph. Model. 2011, 29, 935-946.

26 Hehre, W. J.; Radom, L.; Schleyer, P. V. R.; Pople, J. A. Ab Initio Molecular Orbital Theory; Wiley: NY, 1986.

27 Morris, G. M.; Huey, R.; Lindstrom, W.; Sanner, M. F.; Belew, R. K.; Goodsell, D. S.; Olson, A. J. J. Comput. Chem. 2009, 16, 2785-2791.

28 Pettersen, E. F.; Goddard, T. D.; Huang, C. C.; Couch, G. S.; Greenblatt, D. M.; Meng, E. C.; Ferrin, T. E. J. Comput. Chem. 2004, 25, 1605-1612.

Abstract

An Investigation of *in vitro* Cytotoxicity and apoptotic potential of aromatic diselenides

Masood Ahmad Rizvi,[a]* Santosh Guru,[b] Tahira Naqvi,[a] Manjeet Kumar,[c] Navanath Khumbhar,[d] Showkat Akhoon,[a] Shazia Bhanday,[a] Shashank K. Singh,[b] Shashi Bhushan,[b] G. Mustafa Peerzada,[a] Bhahwal Ali Shah,[c]*

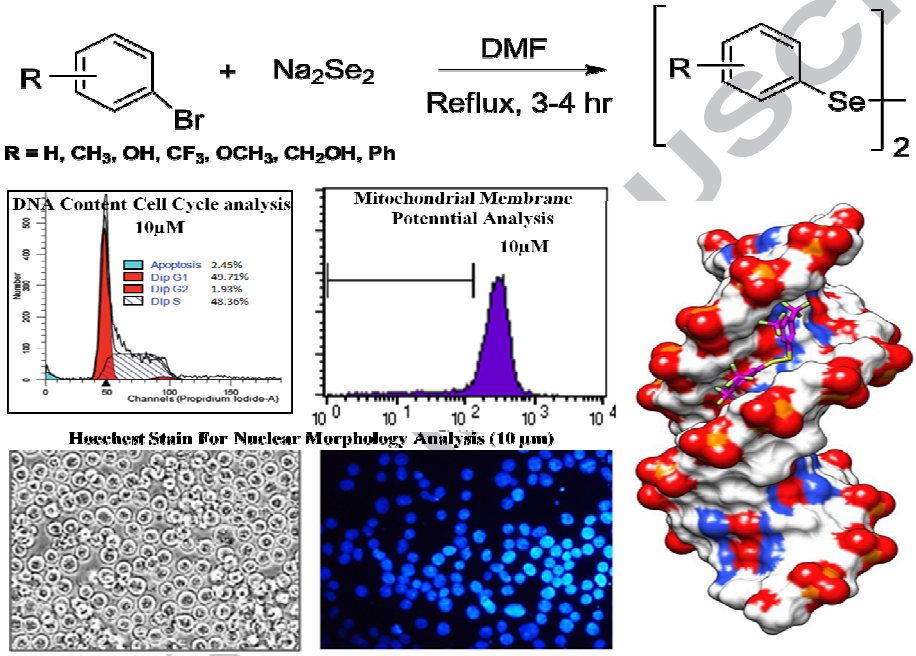

A target synthesis of a library of symmetric aromatic diselenides was attempted with the aim of generating anticancer lead compounds. Out of thirteen screened molecules (**1-13**) against a panel of human cancer cell lines, compound **8** exhibited highest cell growth inhibition in Human leukemia HL-60 cells with IC50 value of 8 µM. Compound **8** had a good pro-apoptotic potential as evidenced from several apoptotic protocols like DNA cell cycle analysis and monitoring of apoptotic bodies formation using phase contrast and nuclear microscopy with Hoechst 33258. Also, **8** significantly inhibits S phase of the cell cycle and eventually trigger apoptosis in HL-60 cells through mitochondrial dependent pathway substantiated by the loss of mitochondrial potential. A theoretical investigation of DNA binding ability of **8** showed that it selectively bind to minor groove of DNA, where it is stabilized by hydrogen bonding and hydrophobic interactions.